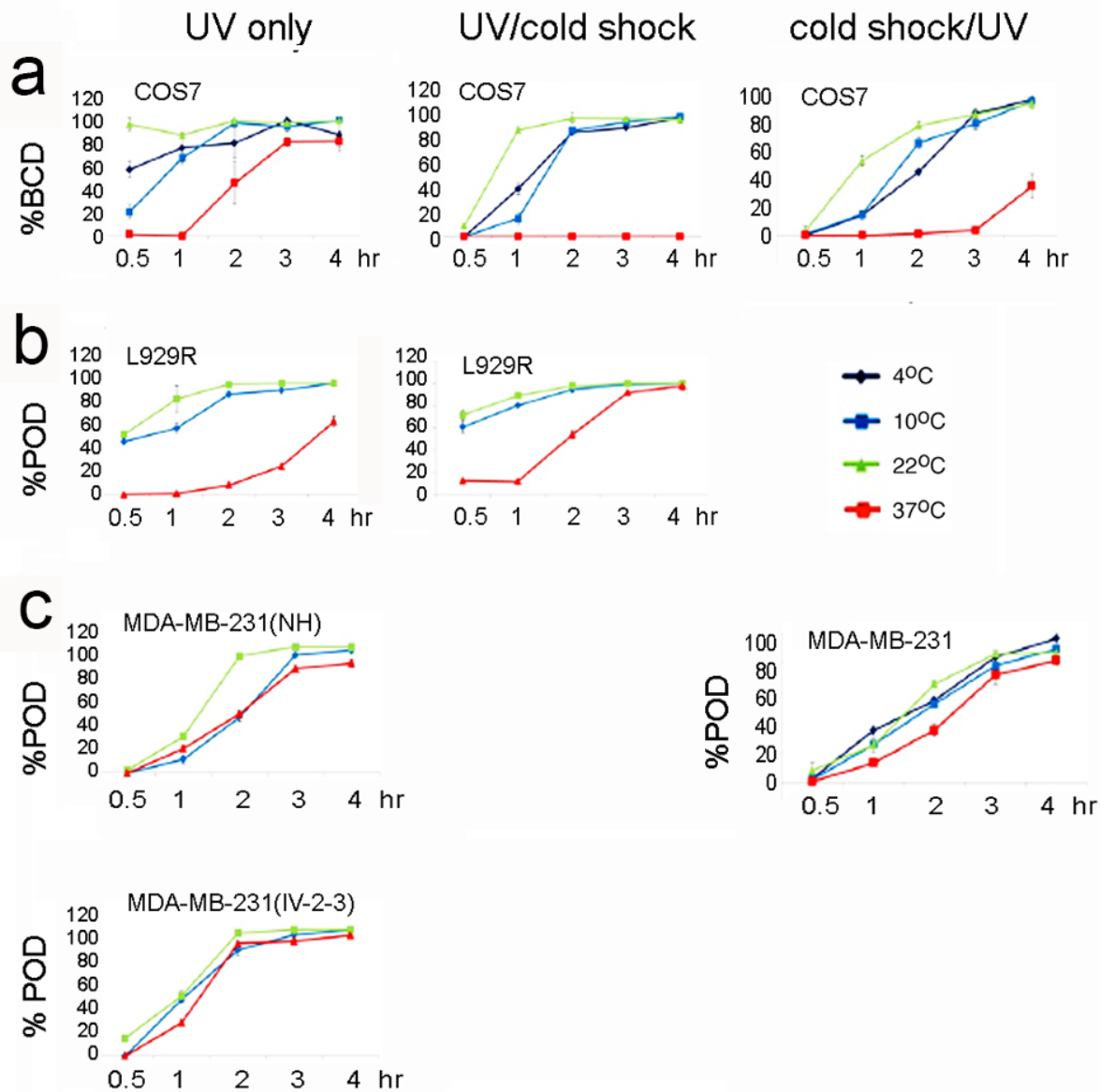


# **WWOX regulates UV/cold shock-mediated calcium influx and nuclear bubbling in frostbite**

Cheng-Chang Tsai<sup>1</sup>, Szu-Jung Chen<sup>1</sup>, Wen-Ting Deng<sup>1</sup>, Tsung-Yun Liu<sup>1</sup>, Kuan-Ting Lee<sup>1</sup>, Ming-Hui Lee<sup>1</sup>, Sing-Ru Lin<sup>1</sup>, Yu-An Chen<sup>1</sup>, Lu-Hai Wang<sup>2</sup>, Li-Jen Su<sup>3</sup>, Hamm-Ming Sheu<sup>4</sup>, and Nan-Shan Chang<sup>1,5,\*</sup>

<sup>1</sup>Institute of Molecular Medicine, College of Medicine, National Cheng Kung University, Tainan, Taiwan, ROC.

## SUPPLEMENTARY INFORMATION

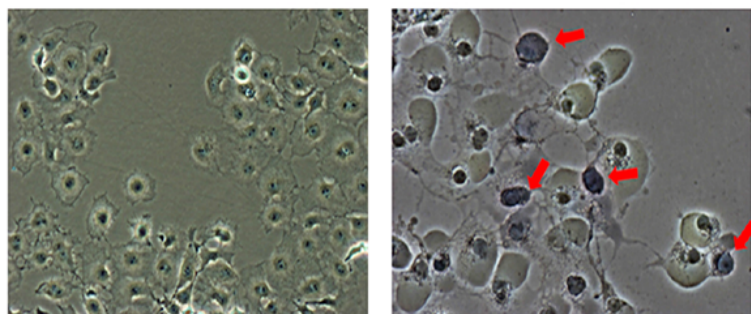
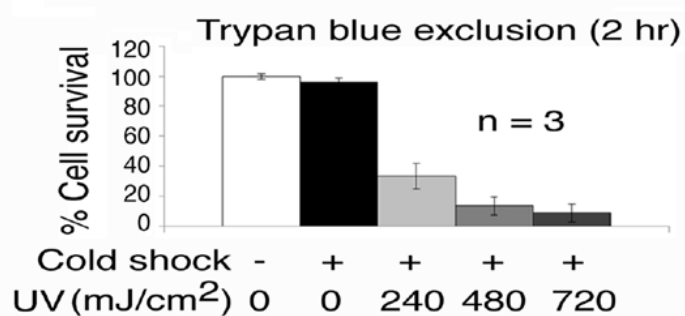
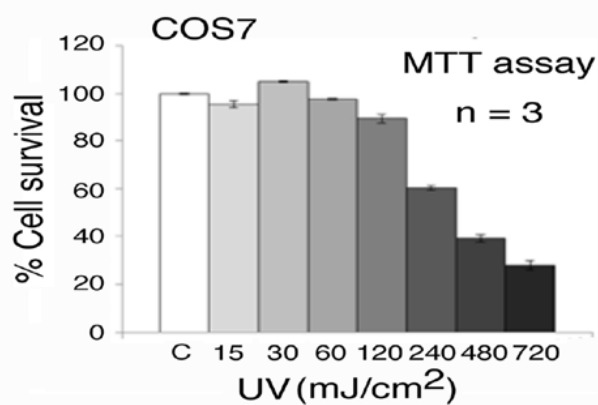
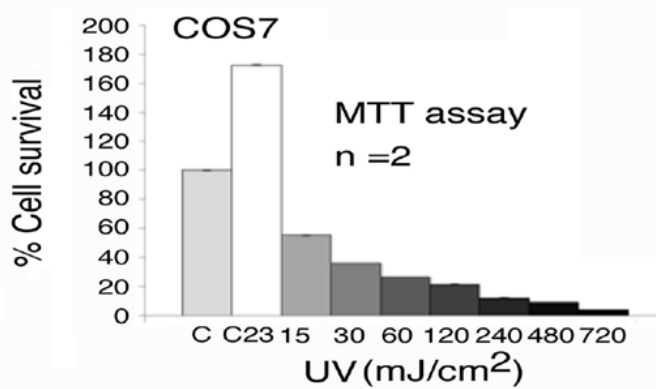


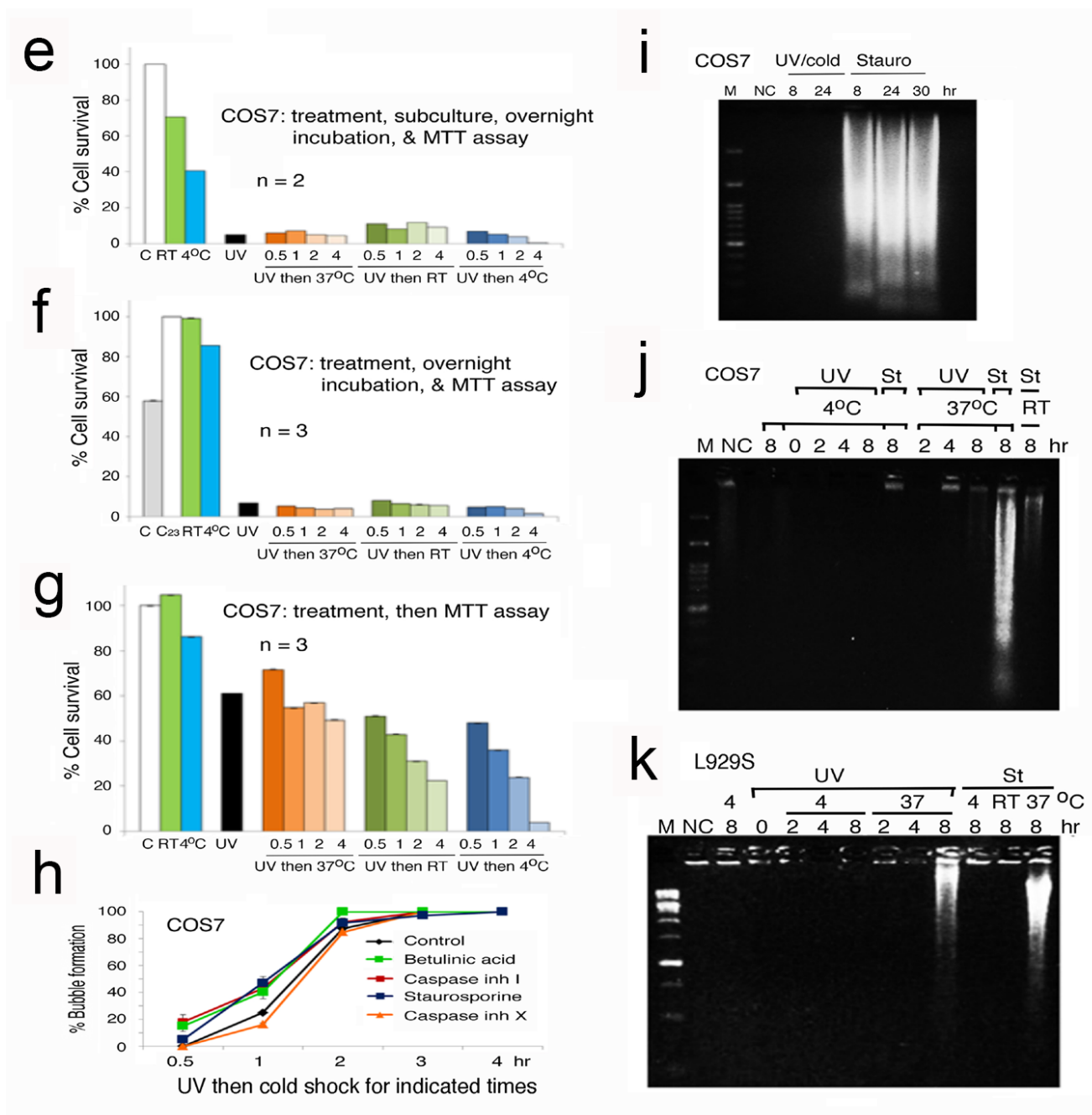
**Supplementary Figure 1. BCD: Nuclear bubbling-induced cell death. a** WWOXf COS7 cells were exposed to UV (480 mJoule/cm<sup>2</sup>) only, UV and then and cold shock (4°C for 5 min), or cold shock and then UV. The cells were then incubated at an indicated temperature for 30 min to 4 hr. % BCD is shown (n=3). **b** Under similar conditions, WWOXd L929R cells were treated with UV only, or UV and then cold shock, followed by incubation at indicated temperatures (n=3). **c** WWOXd breast MDA-MB-231 cells were treated with UV only, or cold shock and then UV, followed by incubation at indicated temperatures (n=3).

**a**

COS7

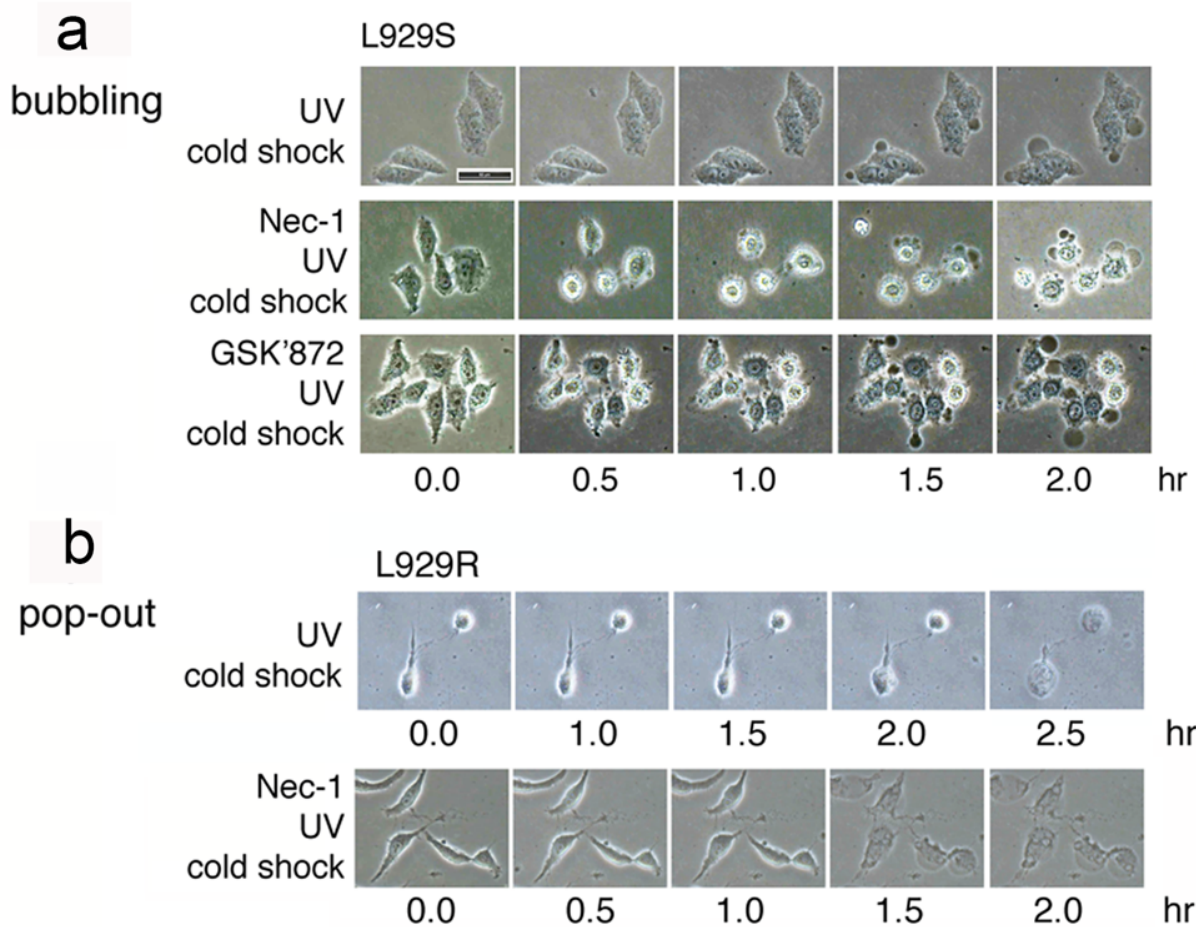
Control      UV then RT 1 hr

**b****c****d**



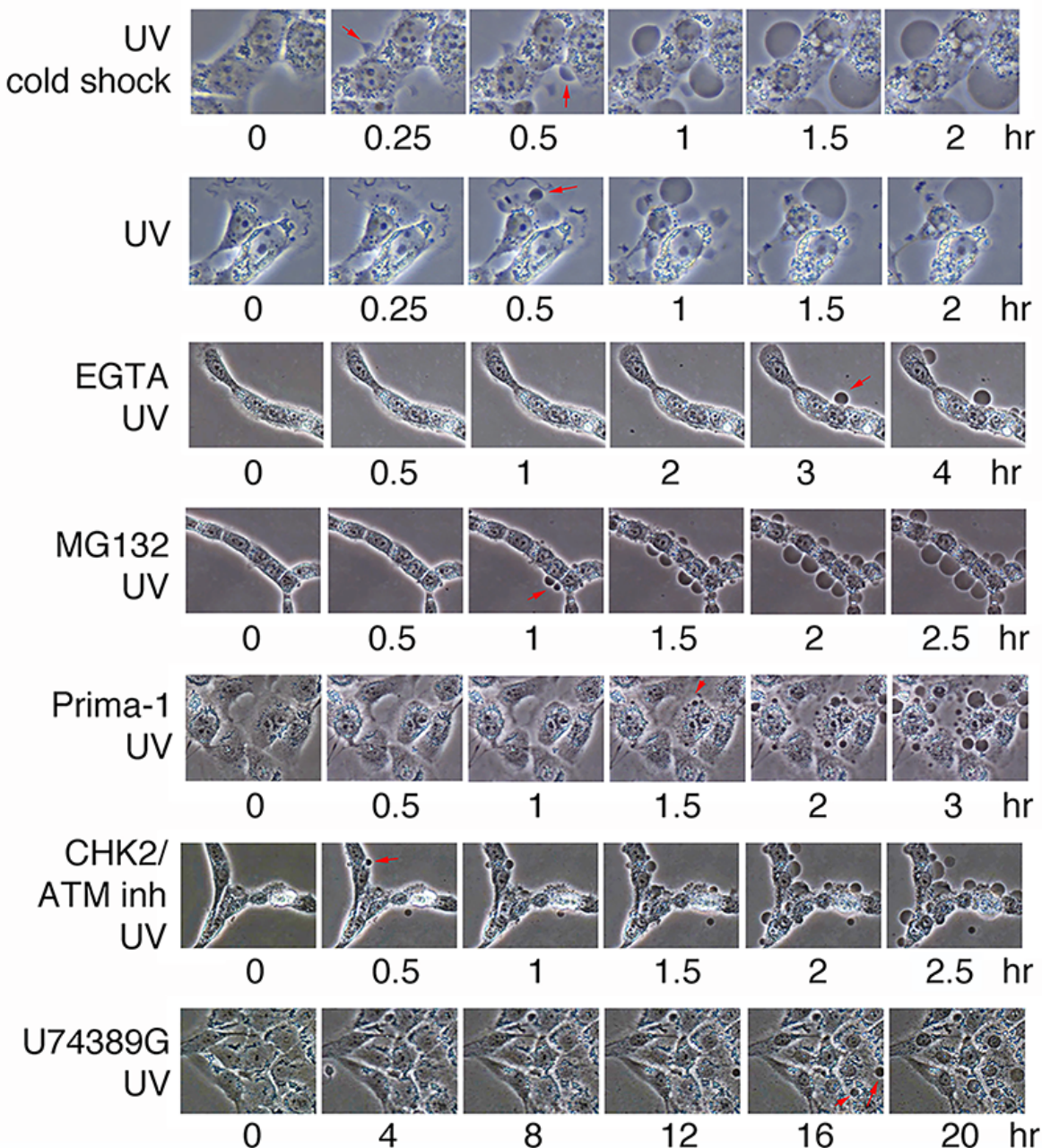
**Supplementary Figure 2. Cellular events in BCD.** **a** COS7 cells were exposed to UV irradiation (480 mJ/cm<sup>2</sup>) and then incubated at room temperature for 1 hour. Failure in trypan blue exclusion is shown in many bubbling cells (red arrows). **b** Similarly, COS7 cells were treated with UV irradiation, followed by cold shock for 5 min and then incubation at room temperature up to 2 hours (mean  $\pm$  standard deviation; n=3). **c** Immediately after UV irradiation, COS7 cells were examined for their survival by MTT assay. **d** Alternatively, UV-irradiated cells were cultured at 37°C for 23 hr, followed by MTT assay. C23 bar = cells received no UV irradiation. **e-g** COS7 cells were exposed to UV and then incubated at 4, 22, or 37°C for indicated times (hr), followed by subculture and incubation at 37°C overnight (e), or incubation at

37°C overnight without subculture (**f**), or without overnight incubation (**g**). The cells were subjected to MTT assays. **h** COS7 cells were treated with 10  $\mu$ M of an indicated chemical for 1 hour, followed by UV and subsequent cold shock at 4°C for indicated times. **i-k** No DNA fragmentation was observed after exposure of COS7 and L929S to UV/cold shock, UV alone, or cold shock alone, and then incubation at 4°C for indicated times. When L929S cells received UV or staurosporine treatment and were then cultured at 37°C for 8 hr, these cells exhibited DNA fragmentation. Staurosporine, at 1  $\mu$ M, induced DNA fragmentation at 37°C but not at room temperature. St or Stauro = Staurosporine; M = DNA markers; NC = non-treated controls.

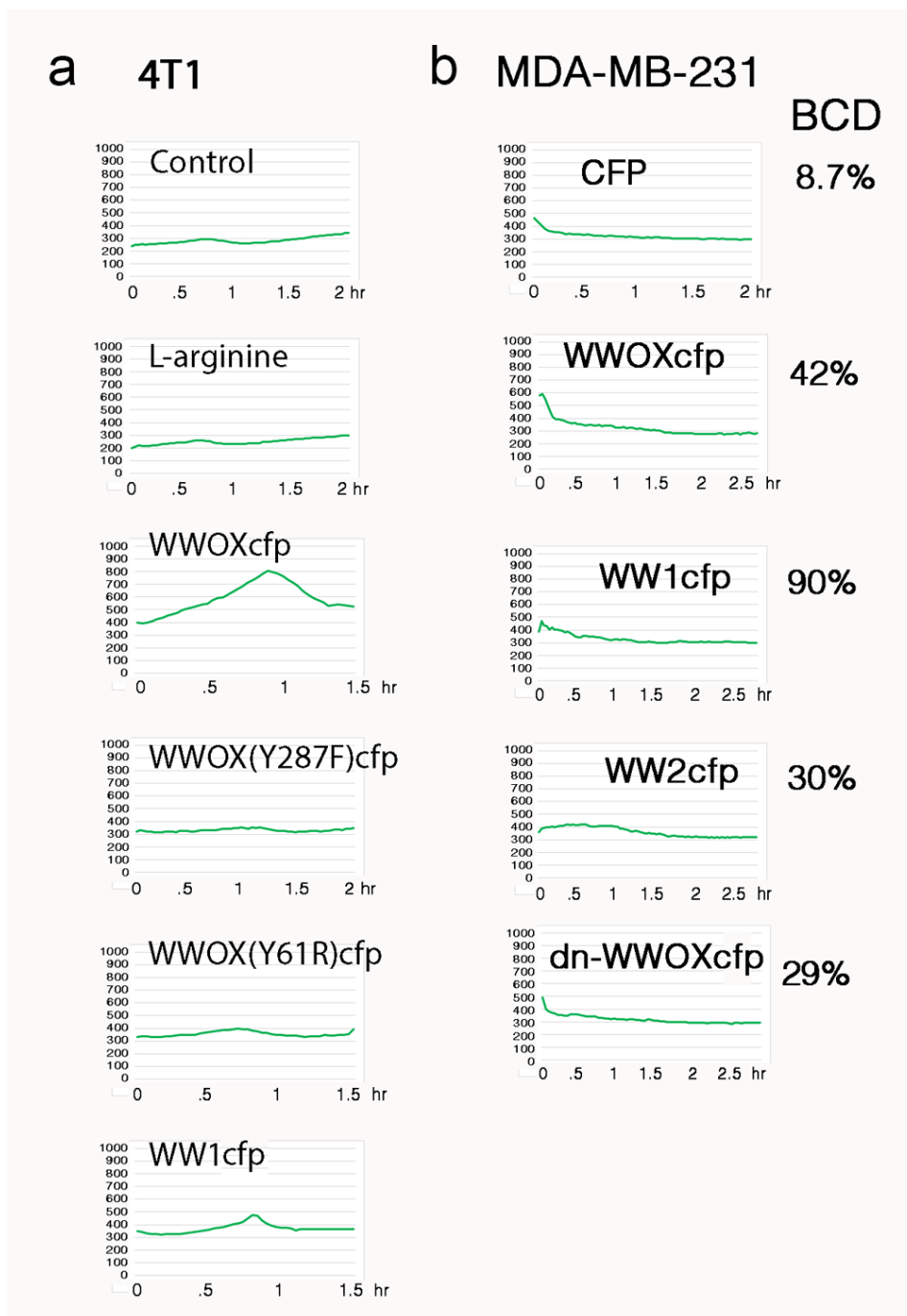


**Supplementary Figure 3. Necroptosis inhibitors cannot block BCD in L929S and POD in L929R cells.** **a** L929S cells were pretreated with Nec-1 or GSK'72 (30  $\mu$ M for 60 min), followed by exposure to UV (480 mJoule/cm<sup>2</sup>). GSK'72 reduced the time for the first appearance of nuclear bubbling by 1 hour in L929S cells. **b** Similarly, L929R cells were pretreated with Nec-1, followed by exposure to UV (480 mJoule/cm<sup>2</sup>). Nec-1 reduced the time for the first appearance of pop-out explosion by 1 hour in L929R cells.

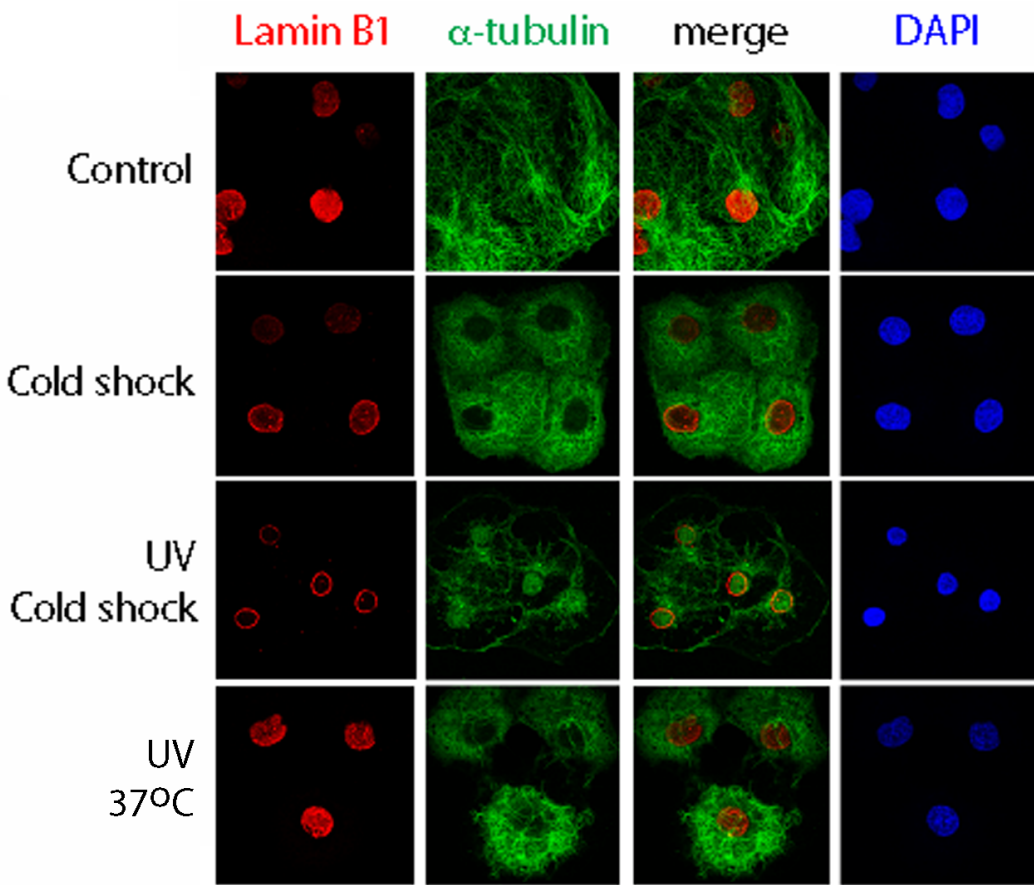
## SCC15



**Supplementary Figure 4. U74389G dramatically suppresses BCD at room temperature.** SCC15 cells were pretreated with EGTA (1 mM), MG132 (30  $\mu$ M), Prima-1 (30  $\mu$ M), CHK2/ATM inhibitor (30  $\mu$ M), or U743890 (30  $\mu$ M) for 30 min. The cells were then subjected to UV irradiation (480 mJoule/cm<sup>2</sup>) or UV/cold shock (5 min at 4°C), followed by examining bubbling by time-lapse microscopy at room temperature. The red arrow indicates the time needed for the first bubble to show up.



**Supplementary Figure 5. Ectopic WWOX restores calcium influx and nuclear bubbling in WWOXd cells.** **a** 4T1 breast cancer cells were transiently overexpressed with a WWOX full-length or other expression constructs. The full-length WWOX restored calcium influx in 4T1 cells. The first WW domain WW1 had a low activity in restoring calcium influx. Y287F and Y61R mutants had no restoring effects. L-arginine at 200  $\mu$ M had no effect. **b** WWOX and other indicated forms failed to restore calcium influx but enabled nuclear bubbling in MDA-MB-231 cells. WW1 had the best activity in promoting nuclear bubbling. dnWWOX is a dominant negative form<sup>21</sup>.



**Supplementary Figure 6. Post UV/cold shock,  $\alpha$ -tubulin is downregulated during continuous culture at 4°C, or is remodeled or conformationally altered during culture at 37°C. COS7 cells were treated with UV (480 mJ/cm<sup>2</sup>) and then cultured at 4 or 37°C for 90 min. Cells were stained with lamin B1 and  $\alpha$ -tubulin for confocal imaging (magnification: 1000X). During subsequent culture at 37°C, the cells underwent apoptosis. The filamentary structure of  $\alpha$ -tubulin was remodeled. At 4°C, the cells underwent BCD.**

# UV480 only Functional Annotation

## Down regulation

Rank	Term	Count	PValue	FDR
1	GO:0006397~mRNA processing	19	1.3E-08	2.0E-05
2	GO:0016071~mRNA metabolic process	20	2.1E-08	3.3E-05
3	GO:0008380~RNA splicing	16	7.5E-08	1.2E-04
4	GO:0051603~proteolysis involved in cellular protein catabolic process	24	6.7E-07	1.1E-03
5	GO:0044257~cellular protein catabolic process	24	7.4E-07	1.2E-03
6	GO:0019941~modification-dependent protein catabolic process	23	1.1E-06	1.7E-03
7	GO:0043632~modification-dependent macromolecule catabolic process	23	1.1E-06	1.7E-03
8	GO:0030163~protein catabolic process	24	1.4E-06	2.1E-03
9	GO:0044265~cellular macromolecule catabolic process	25	1.8E-06	2.9E-03
10	GO:0009057~macromolecule catabolic process	25	6.2E-06	9.9E-03
11	GO:0006396~RNA processing	19	2.2E-05	3.4E-02
12	GO:0010608~posttranscriptional regulation of gene expression	10	1.6E-04	2.6E-01
13	GO:0006325~chromatin organization	14	3.1E-04	4.8E-01
14	GO:0016568~chromatin modification	12	3.2E-04	5.1E-01
15	GO:0051276~chromosome organization	16	3.3E-04	5.3E-01
16	GO:0006417~regulation of translation	8	3.7E-04	5.9E-01
17	GO:0006508~proteolysis	28	5.6E-04	8.8E-01

## Up regulation

Rank	Term	Count	PValue	FDR
1	GO:0006412~translation	19	1.6E-11	2.2E-08
2	GO:0007608~sensory perception of smell	25	1.3E-06	1.8E-03
3	GO:0007606~sensory perception of chemical stimulus	25	4.1E-06	5.6E-03
4	GO:0007186~G-protein coupled receptor protein signaling pathway	30	5.6E-05	7.8E-02
5	GO:0007600~sensory perception	25	6.1E-05	8.4E-02
6	GO:0050890~cognition	25	1.4E-04	2.0E-01
7	GO:0050877~neurological system process	26	3.9E-04	5.4E-01

# 4°C(30 min) Functional Annotation

## Down regulation

Rank	Term	Count	PValue	FDR
1	GO:0007186~G-protein coupled receptor protein signaling pathway	42	1.6E-08	2.3E-05
2	GO:0007608~sensory perception of smell	30	1.1E-07	1.6E-04
3	GO:0007606~sensory perception of chemical stimulus	31	1.2E-07	1.8E-04
4	GO:0007600~sensory perception	32	1.2E-06	1.8E-03
5	GO:0050890~cognition	32	3.9E-06	5.7E-03
6	GO:0007166~cell surface receptor linked signal transduction	43	1.3E-05	1.9E-02
7	GO:0050877~neurological system process	32	5.0E-05	7.3E-02

## Up regulation

Rank	Term	Count	PValue	FDR
1	GO:0007606~sensory perception of chemical stimulus	22	1.1E-02	1.6E+01
2	GO:0050877~neurological system process	28	1.3E-02	1.8E+01
3	GO:0006007~glucose catabolic process	4	1.7E-02	2.3E+01
4	GO:0019320~hexose catabolic process	4	1.7E-02	2.3E+01
5	GO:0046365~monosaccharide catabolic process	4	1.8E-02	2.5E+01
6	GO:0007608~sensory perception of smell	20	2.2E-02	2.9E+01
7	GO:0044275~cellular carbohydrate catabolic process	4	2.4E-02	3.1E+01
8	GO:0046164~alcohol catabolic process	4	3.0E-02	3.7E+01
9	GO:0007600~sensory perception	23	3.2E-02	3.9E+01
10	GO:0043933~macromolecular complex subunit organization	9	3.7E-02	4.4E+01
11	GO:0050708~regulation of protein secretion	3	3.8E-02	4.5E+01
12	GO:0006334~nucleosome assembly	4	4.0E-02	4.6E+01
13	GO:0034621~cellular macromolecular complex subunit organization	7	4.2E-02	4.8E+01
14	GO:0031497~chromatin assembly	4	4.3E-02	4.9E+01
15	GO:0034728~nucleosome organization	4	4.4E-02	5.0E+01

# UV480 mJ/cm<sup>2</sup> + 4°C(30min)

## Functional Annotation

### Down regulation

Rank	Term	Count	PValue	FDR
1	GO:0006397~mRNA processing	19	4.9E-08	7.9E-05
2	GO:0016071~mRNA metabolic process	20	8.2E-08	1.3E-04
3	GO:0008380~RNA splicing	16	2.3E-07	3.7E-04
4	GO:0051603~proteolysis involved in cellular protein catabolic process	23	1.0E-05	1.6E-02
5	GO:0044257~cellular protein catabolic process	23	1.1E-05	1.8E-02
6	GO:0043632~modification-dependent macromolecule catabolic process	22	1.5E-05	2.5E-02
7	GO:0019941~modification-dependent protein catabolic process	22	1.5E-05	2.5E-02
8	GO:0030163~protein catabolic process	23	1.9E-05	3.0E-02
9	GO:0044265~cellular macromolecule catabolic process	24	2.5E-05	4.1E-02
10	GO:0010608~posttranscriptional regulation of gene expression	11	5.9E-05	9.5E-02
11	GO:0006396~RNA processing	19	6.7E-05	1.1E-01
12	GO:0009057~macromolecule catabolic process	24	7.5E-05	1.2E-01
13	GO:0034622~cellular macromolecular complex assembly	13	7.7E-05	1.2E-01
14	GO:0006417~regulation of translation	9	1.0E-04	1.6E-01
15	GO:0034621~cellular macromolecular complex subunit organization	13	2.4E-04	3.9E-01

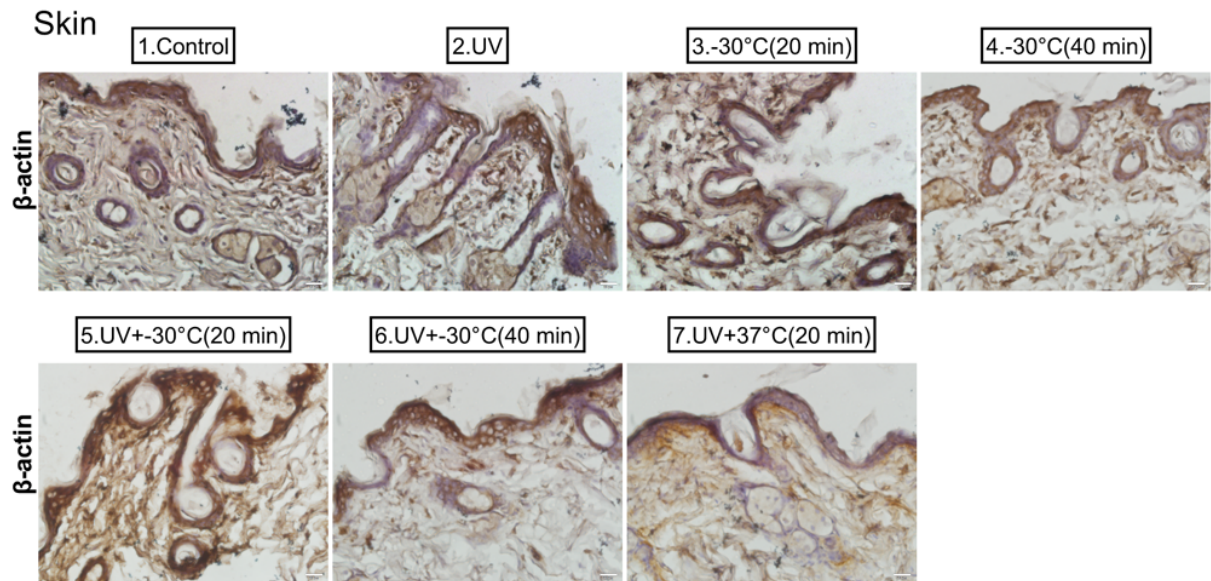
# UV480 mJ/cm<sup>2</sup> + 4°C(30min) Functional Annotation

## Up regulation

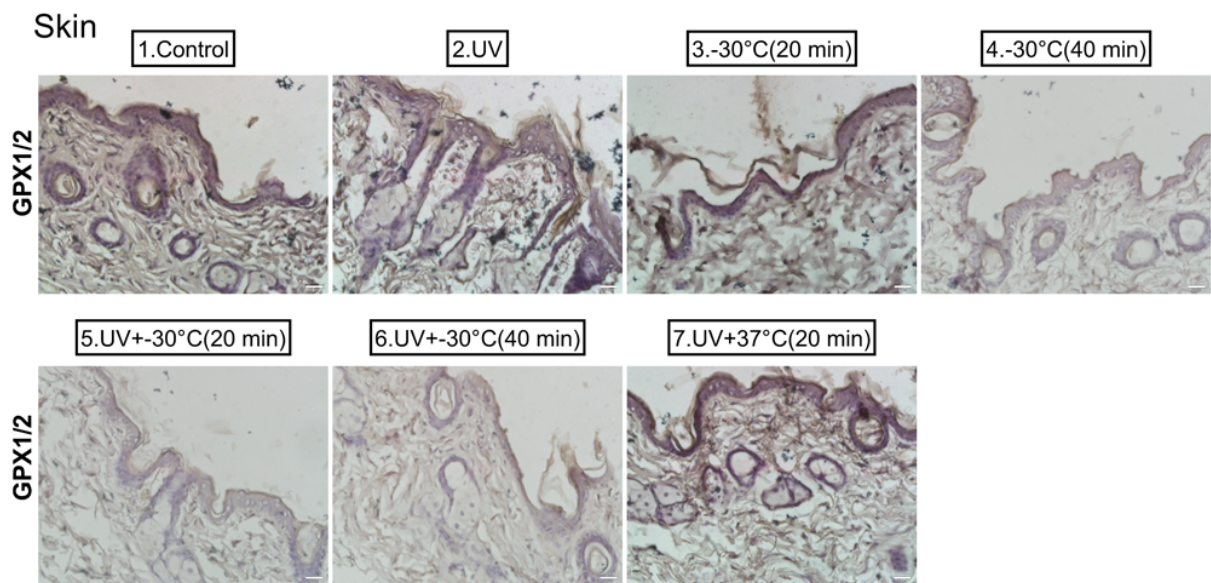
Rank	Term	Count	PValue	FDR
1	GO:0007608~sensory perception of smell	25	2.0E-07	2.8E-04
2	GO:0007606~sensory perception of chemical stimulus	25	6.6E-07	9.1E-04
3	GO:0007186~G-protein coupled receptor protein signaling pathway	32	7.6E-07	1.0E-03
4	GO:0006412~translation	13	1.4E-06	1.9E-03
5	GO:0007600~sensory perception	25	1.1E-05	1.6E-02
6	GO:0050890~cognition	25	2.8E-05	3.9E-02
7	GO:0007166~cell surface receptor linked signal transduction	33	1.0E-04	1.4E-01
8	GO:0050877~neurological system process	25	2.1E-04	2.9E-01

**Supplementary Figure 7. Gene expression profiles of L929S cells upon exposure to UV (480 mJoule/cm<sup>2</sup>) and/or cold shock at 4°C for 30 min.** 6 Gene chips from Affymetrix were used.

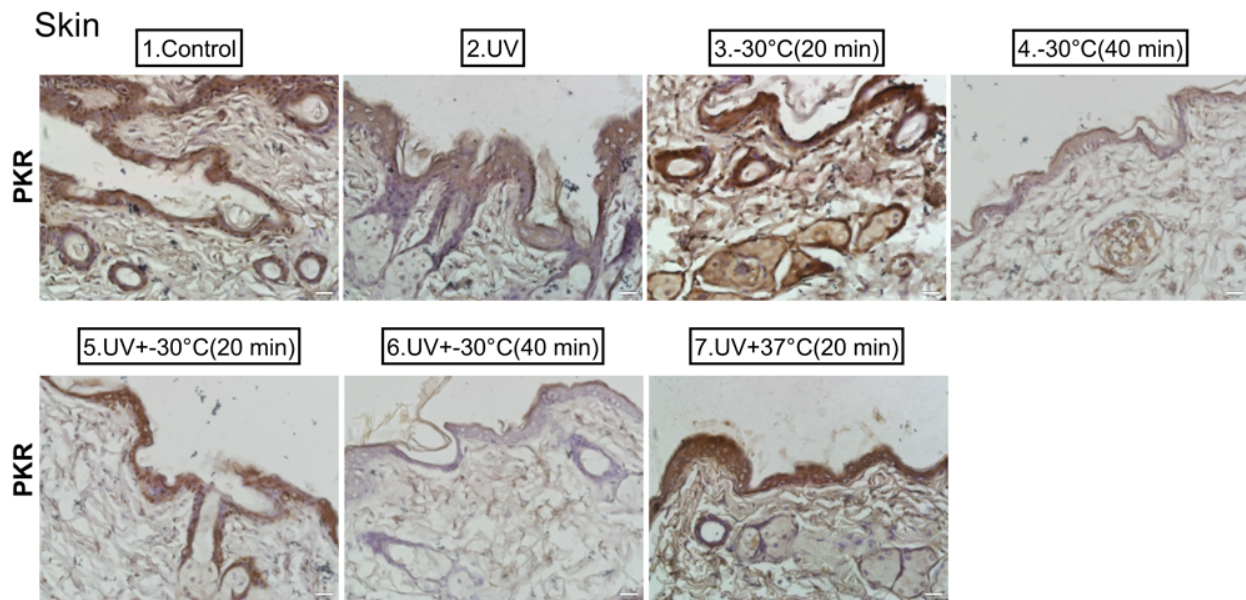
**a**



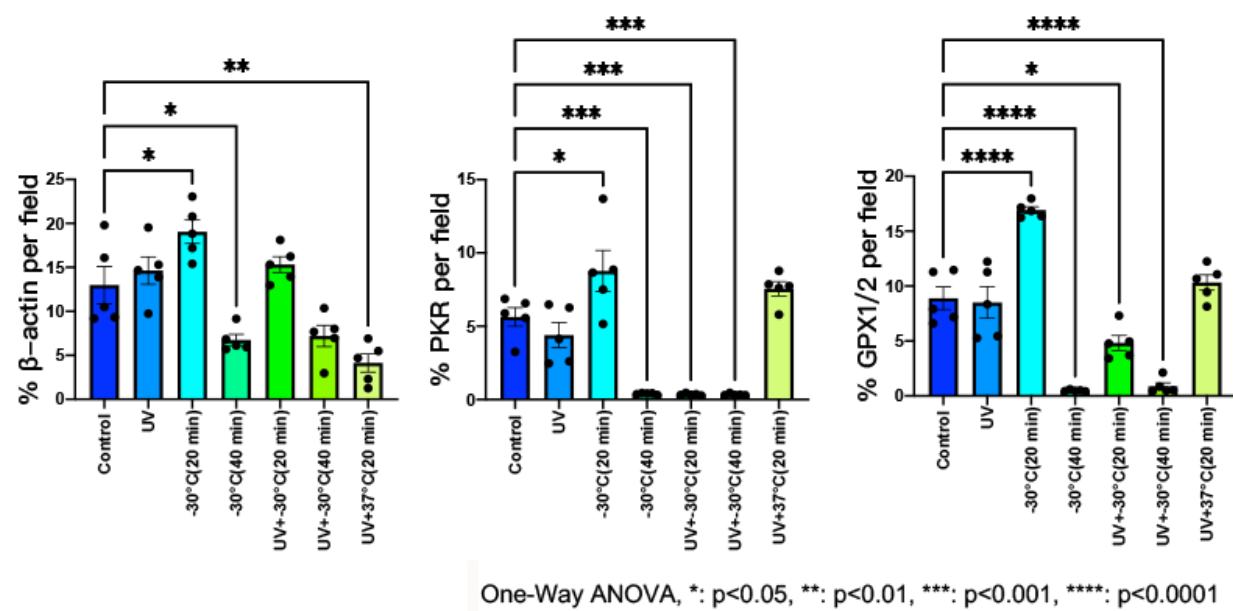
**b**



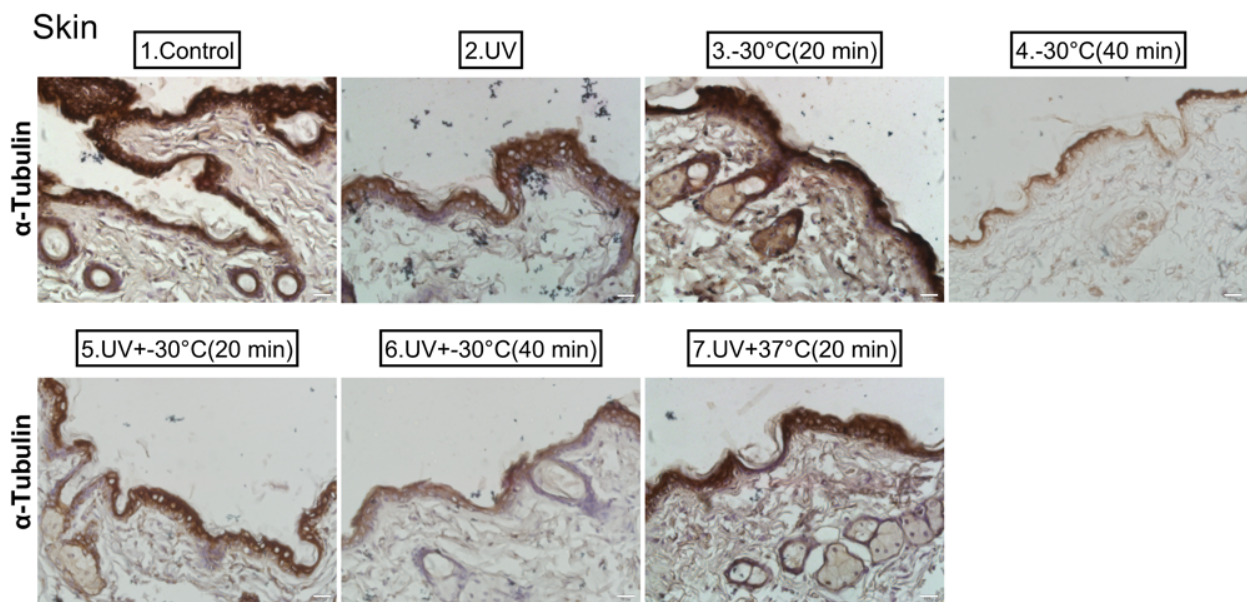
C



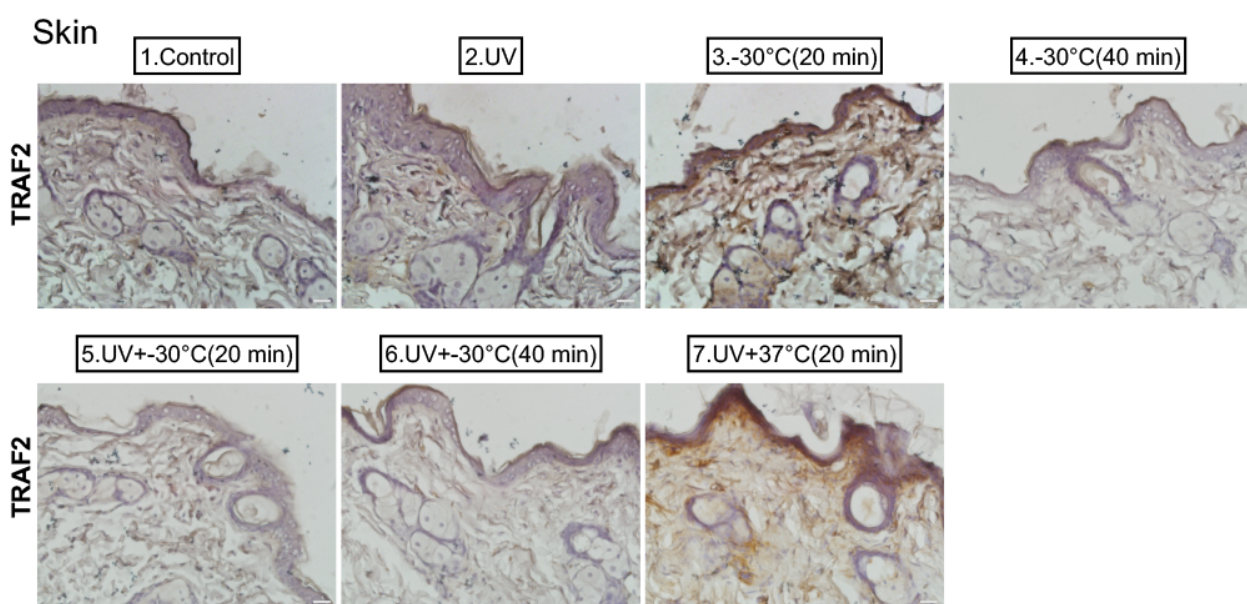
D



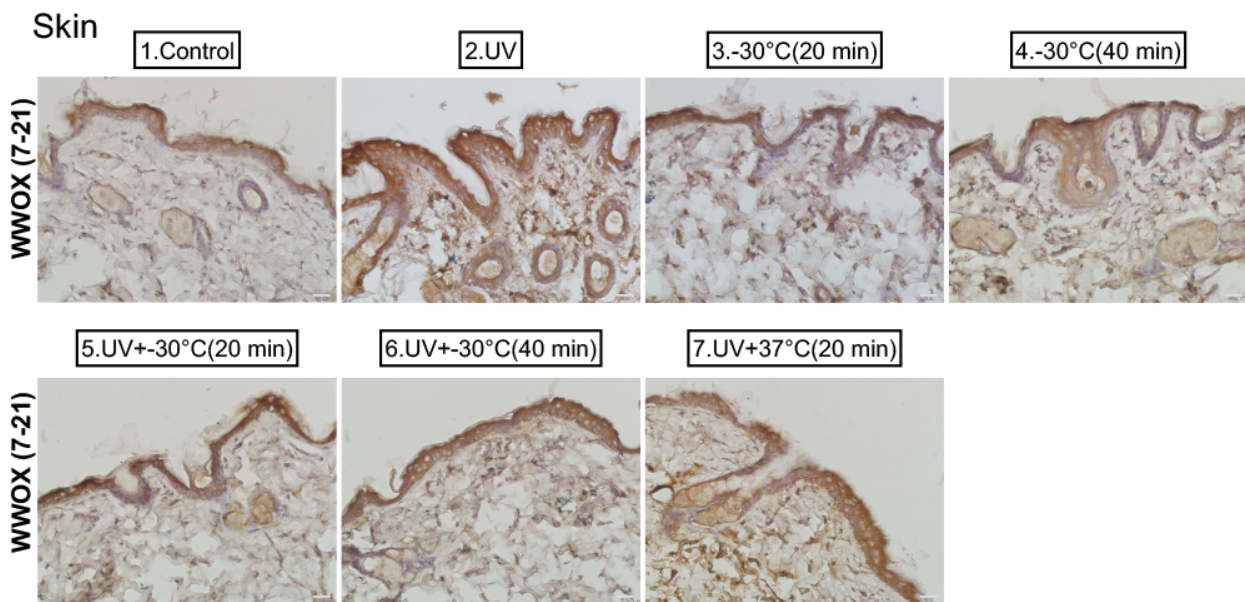
e



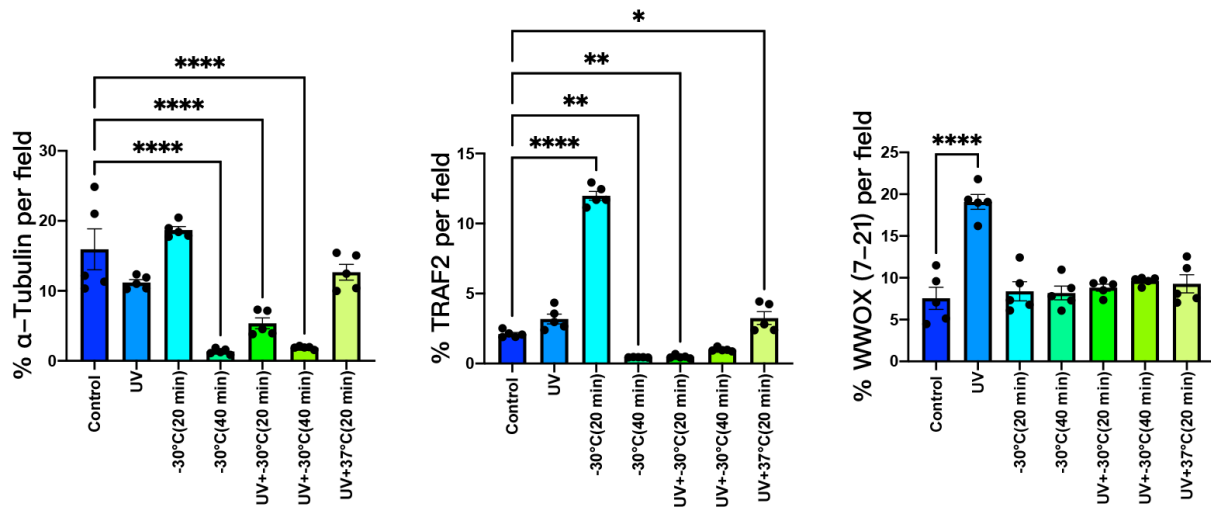
f



g

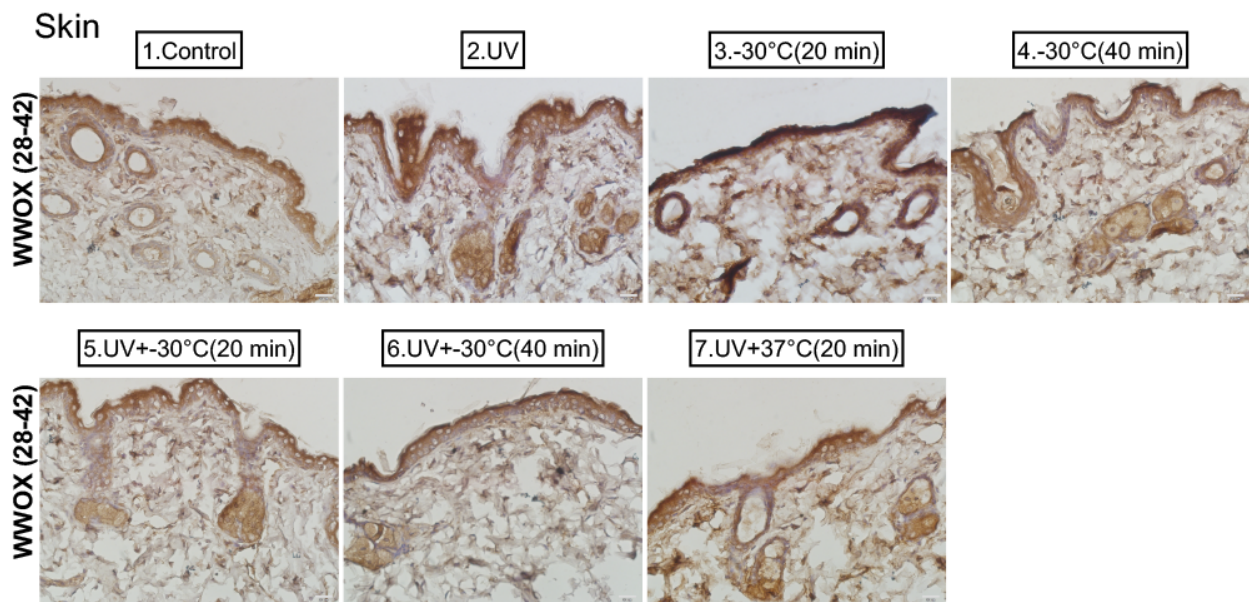


h

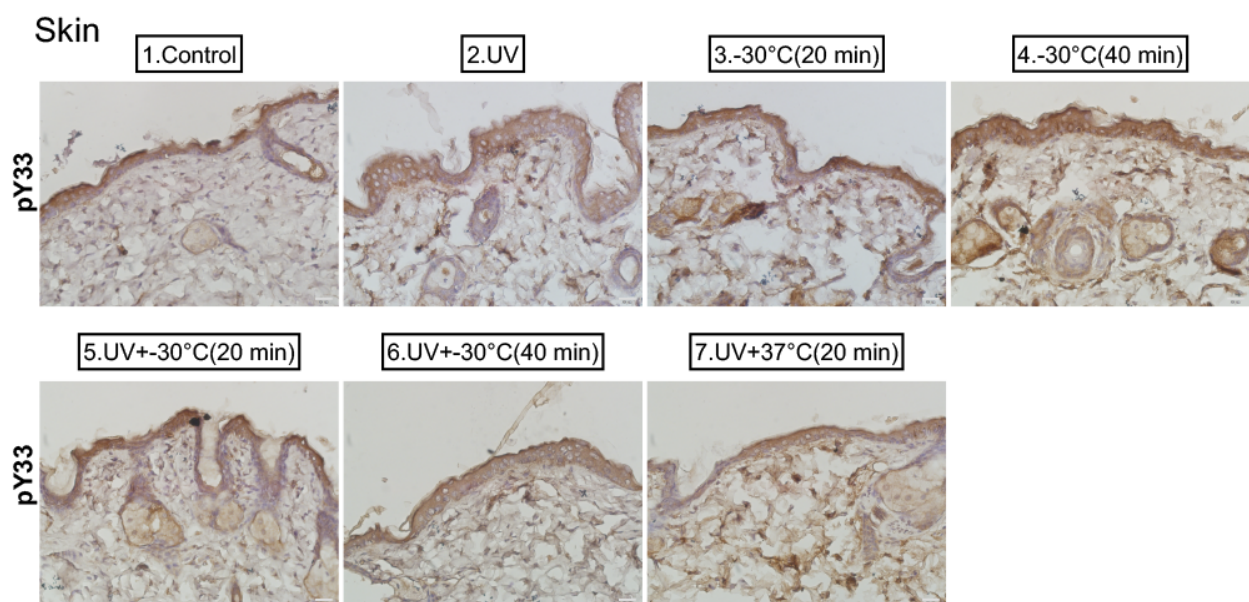


One-Way ANOVA, \*: p<0.05, \*\*: p<0.01, \*\*\*: p<0.001, \*\*\*\*: p<0.0001

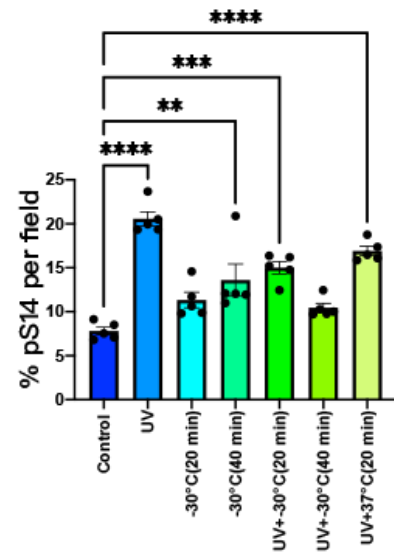
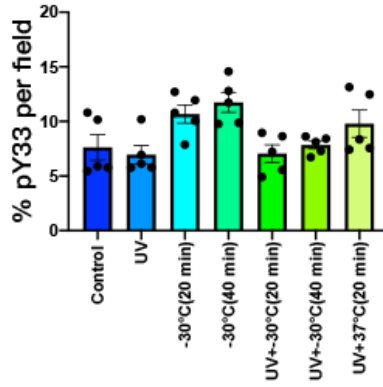
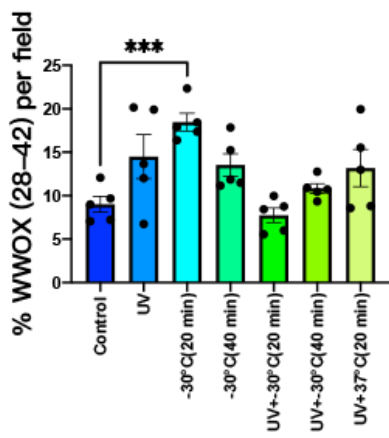
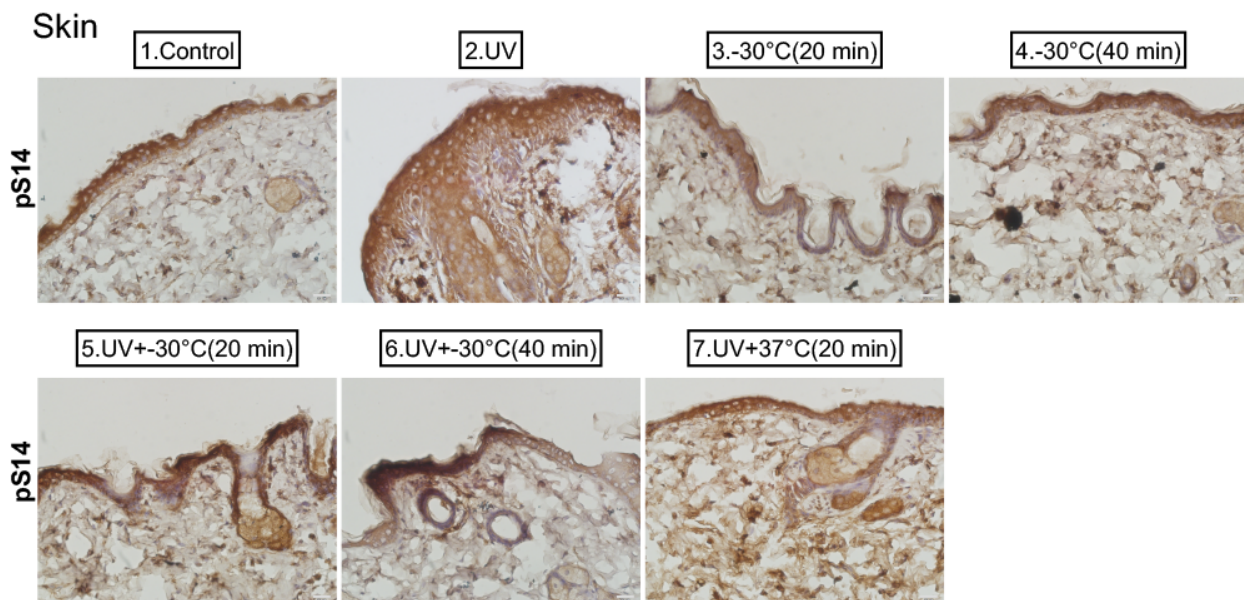
i



j



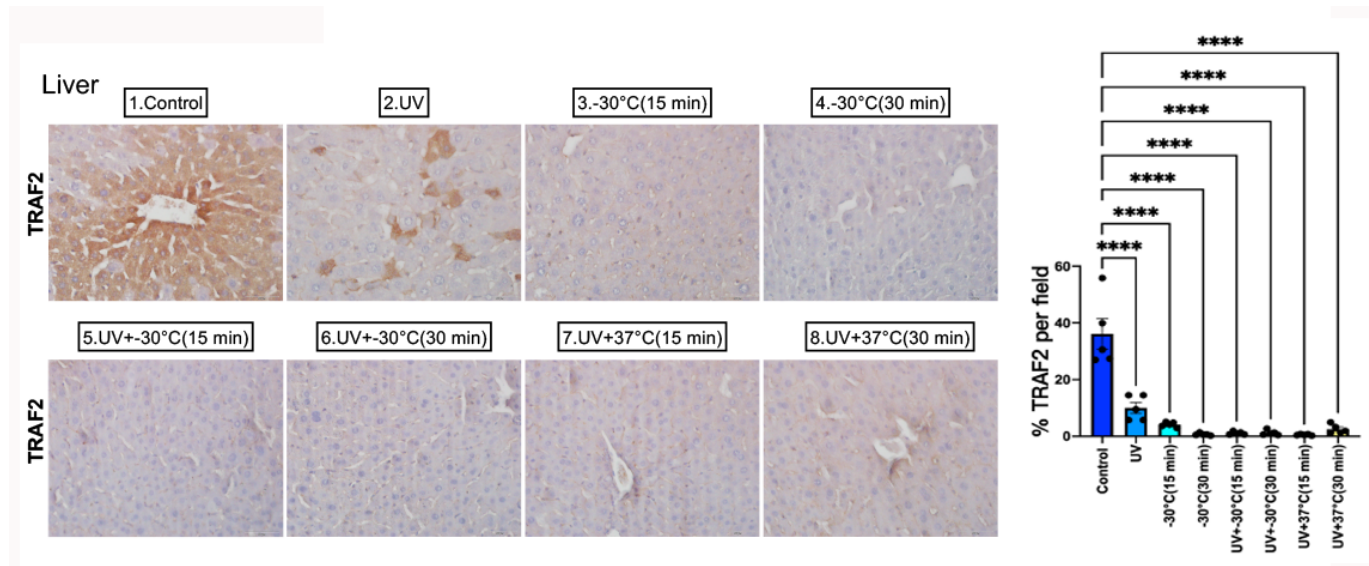
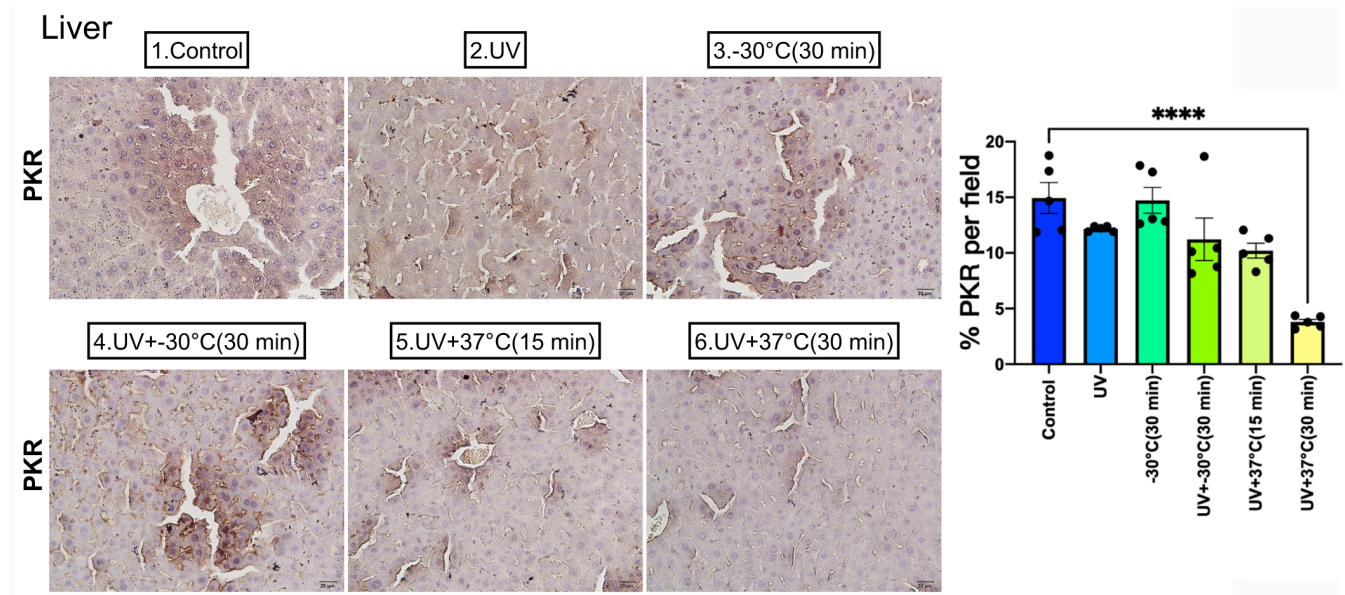
K

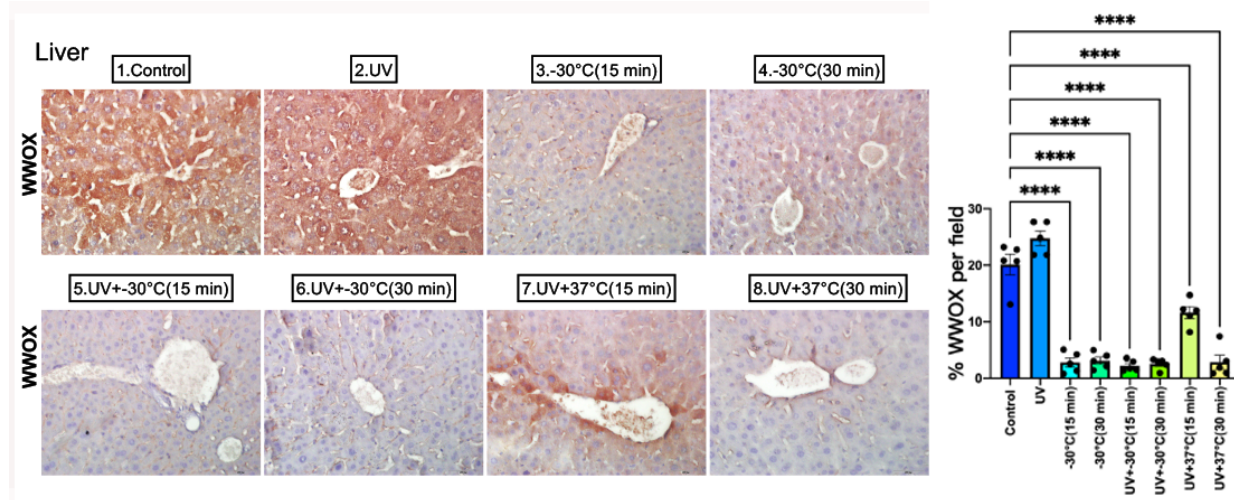
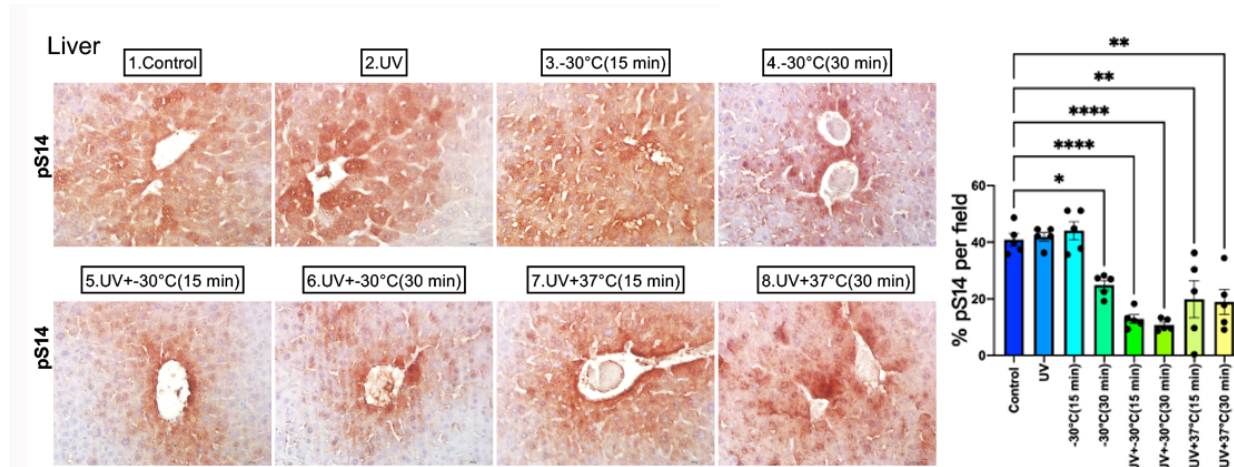
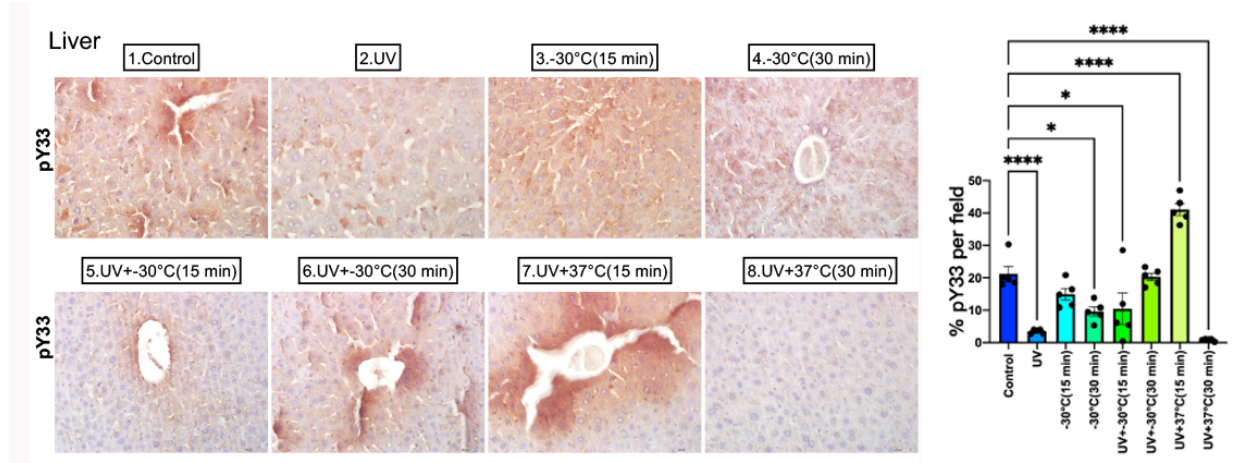


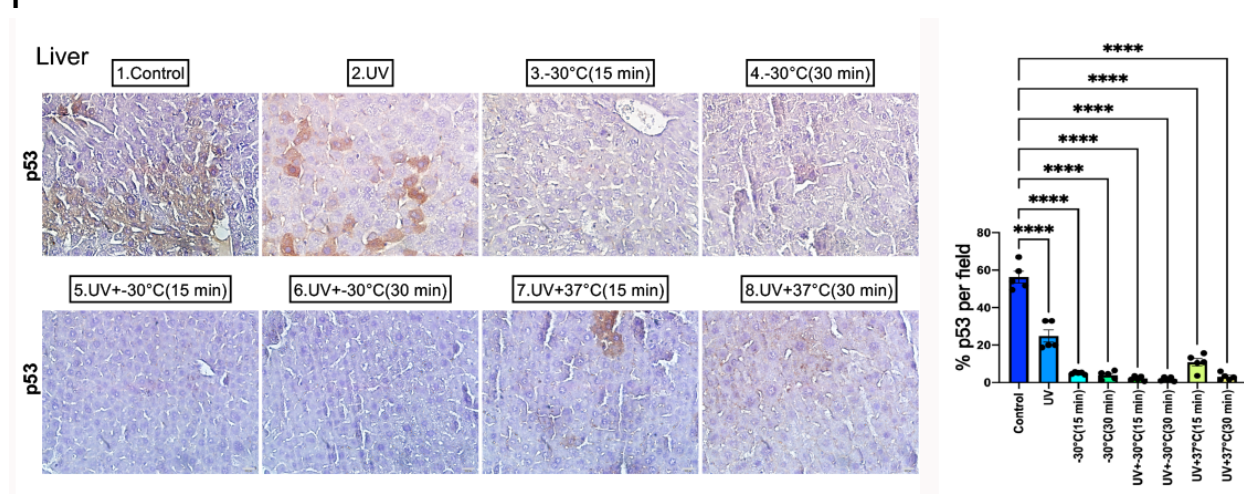
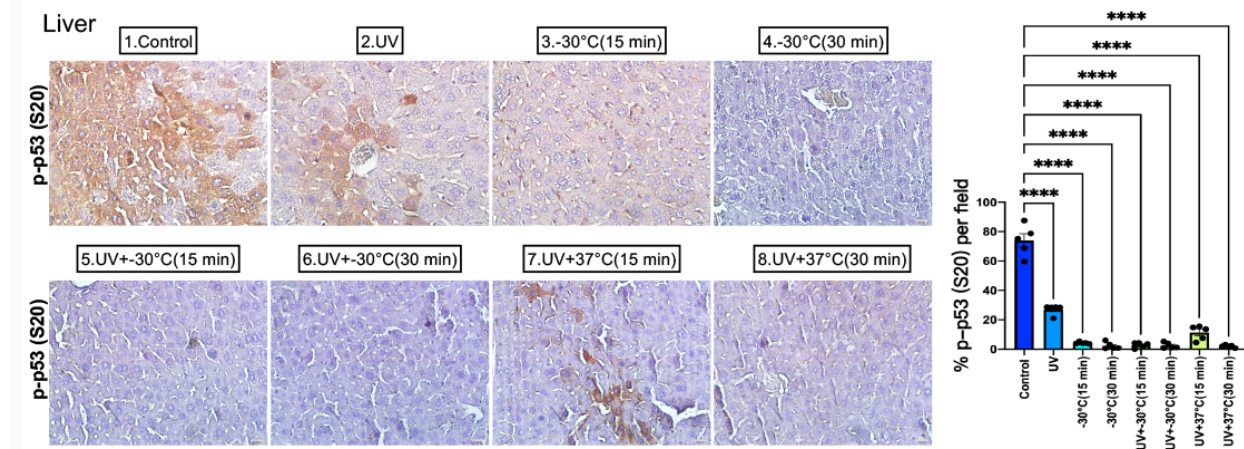
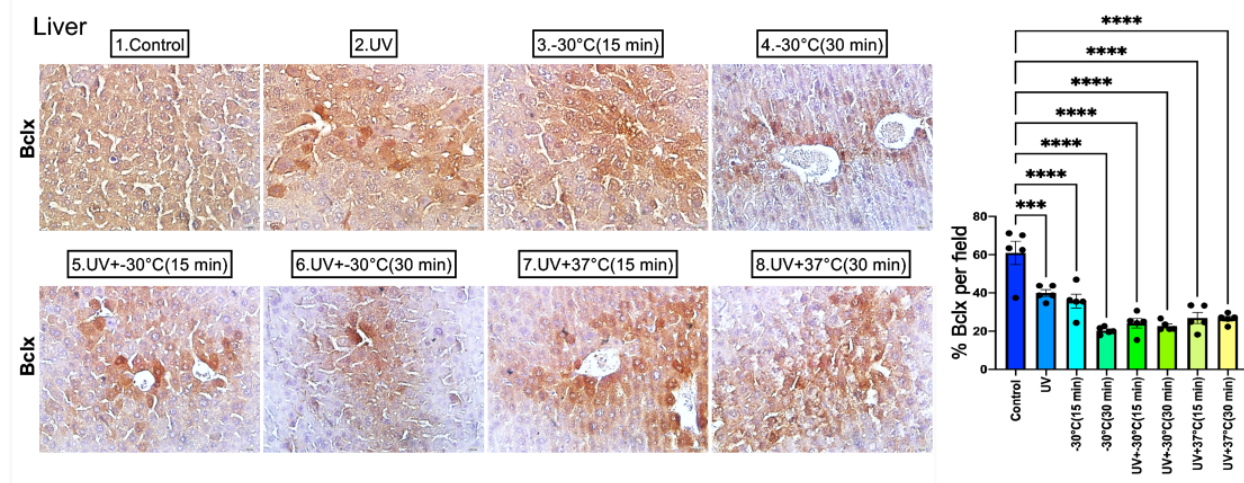
One-Way ANOVA, \*: p<0.05, \*\*: p<0.01, \*\*\*: p<0.001, \*\*\*\*: p<0.0001

**Supplementary Figure 8. Protein expression in the skin of UV/cold shock-treated hairless mice. a-l**

Mice were exposed to UV (960 mJoule/cm<sup>2</sup>) and/or cold shock in a -30°C cold box for 20 and 40 min, respectively. Alternatively, mice were exposed to UV and then placed in a 37°C chamber for 20 min. Post experiments, mice were sacrificed. IHC was carried to determine protein expression in the skin using specific antibodies. Antibodies against WWOX amino acid segments at 7-21 (g) and 28-42 (i) were used, respectively. One way ANOVA was used to analyze the statistical differences among all samples in each experimental group (n=5; \*p<0.05; \*\*p<0.01; \*\*\*p<0.001; \*\*\*\*p<0.0001).

**a****b**

**C****d****e**

**f****g****h**

i

Liver



Negative control (no primary antibody)  
(40x magnification)

**Supplementary Figure 9. Protein expression in liver in UV/cold shock-treated hairless mice. a-i**  
Hairless mice were exposed to UV ( $960 \text{ mJ/cm}^2$ ) and then temperature shocked at  $-30^\circ\text{C}$  or  $37^\circ\text{C}$  for 15 and 30 min, respectively. The mice were then sacrificed. By immunohistochemistry, expression of TRAF2, PKR, WWOX and phosphorylation at S14 or Y33, p53 and phosphorylation at S20, and Bcl-x is shown. One way ANOVA was used to analyze the statistical differences among all samples in each experimental group ( $n=5$ ;  $*p<0.05$ ;  $**p<0.01$ ;  $***p<0.001$ ;  $****p<0.0001$ ).

## SUPPLEMENTAL VIDEO

### **Supplementary Video 1. UV/cold shock-induced bubbling cell death (BCD) in MCF7 cells.**

Breast MCF7 cells were exposed to UV irradiation (480 mJoule/cm<sup>2</sup>) and cold shock for 5 min at 4°C, and then subjected to time-lapse microscopy at RT (2 min per frame). 200x magnification. Cells were labeled with DAPI, PI and Fluo-8 (green) for imaging nuclei in blue, nuclei in red, and calcium influx in green, respectively.

### **Supplementary Video 2. UV/cold shock-induced pop-out explosion death (POD) in breast MDA-MB-231 cells.**

MDA-MB-231 cells were exposed to UV irradiation (480 mJoule/cm<sup>2</sup>) and cold shock for 5 min at 4°C, and then subjected to time-lapse microscopy at RT (2 min per frame). 200x magnification. Cells were labeled with DAPI, PI and Fluo-8 (green) for imaging nuclei in blue, nuclei in red, and calcium influx in green, respectively.

### **Supplementary Videos 3 and 4. Time-lapse holographic microscopy of UV/cold shock-induced BCD in COS7 cells.**

Experiments were carried out at 4°C in UV/cold shock-treated COS7 cells at 100x (S3) and 400x (S4) magnifications, respectively.

### **Supplementary Video 5. Time-lapse holographic microscopy of UV/cold shock-induced BCD in L929S cells.**

The experiment was carried out at 4°C using UV/cold shock-treated L929S cells (400x magnification).

### **Supplementary Video 6. Time-lapse holographic microscopy of staurosporine-induced apoptosis in L929S cells.**

The experiment was carried out at 37°C using staurosporine (2 μM)-treated L929S (400x magnification).

### **Supplementary Video 7. Time-lapse holographic microscopy of UV/cold shock-treated L929S cells culturing at 37°C.**

when UV/cold-shock-treated L929S cells were cultured at 37°C, apoptosis occurred and the cell bubble heights reaching ~ 15 μm (Video S7).

### **Supplementary Videos 8 and 9. Time-lapse holographic microscopy of L929S cell proliferation.**

Experiments were carried out at 37°C to image L929S cell division (400x magnification) in duplicates.

### **Supplementary Video 10. Time-lapse fluorescent microscopy of 4T1-WWOXcfp cells: green calcium influx channel.**

4T1 breast cancer cells were transiently overexpressed with WWOXcfp full-length, treated with UV (960 mJoule/cm<sup>2</sup>), and imaged at room temperature. Cells were stained with fluo-8 for calcium influx, and DAPI and PI for nuclei. Only data for calcium influx is shown (200x magnification). A sphere and surrounding cells were imaged.

### **Supplementary Video 11. Time-lapse fluorescent microscopy of 4T1-WWOXcfp cells: cfp channel.**

4T1 breast cancer cells were transiently overexpressed with WWOXcfp full-length, treated with UV (960 mJoule/cm<sup>2</sup>), and imaged at room temperature. Cells were stained with fluo-8 for calcium influx, DAPI and PI for nuclei. Only data for cfp is shown (200x magnification). A sphere and surrounding cells were imaged.

**Supplementary Video 12. Time-lapse fluorescent microscopy of 4T1-CFP cells: green calcium influx channel.** 4T1 breast cancer cells were transiently overexpressed with cfp, treated with UV (960 mJoule/cm<sup>2</sup>), and imaged at room temperature. Cells were stained with fluo-8 for calcium influx, and DAPI and PI for nuclei. Only data for calcium influx is shown (200x magnification).

**Supplementary Video 13. Time-lapse fluorescent microscopy of 4T1-CFP cells: cfp channel.** 4T1 breast cancer cells were transiently overexpressed with cfp, treated with UV (960 mJoule/cm<sup>2</sup>), and imaged at room temperature. Cells were stained with fluo-8 for calcium influx, and DAPI and PI for nuclei. Only data for cfp is shown (200x magnification).